The 2016 World Congress on
Advances in Civil, Environmental, and Materials Research (ACEM16)
Jeju Island, Korea, August 28-September 1, 2016

Frequency and temperature dependent electro active regions in $SrMnO_3$

*Shahid Atiq[1)], S. Kumail Abbas[2)], Saira Riaz[3)] and Shahzad Naseem[4)]

[1), 2), 3), 4)] *Centre of Excellence in Solid State Physics, University of the Punjab, Quaid-e-Azam Campus, Lahore-54590, Pakistan*
[1)] *satiq.cssp@pu.edu.pk*

ABSTRACT

A series of $SrMnO_3$ ceramics was prepared by sol-gel auto-combustion route and subsequently sintered at various temperatures ranging from 600 to 1200 °C in order to optimize the conditions for a phase pure synthesize of the samples. X-ray diffraction confirmed the single phase nature of the sample sintered at 1000 °C for 4 hrs. Refined information regarding the structural parameters of the prepared samples was achieved via Rietveld's refinement. The effect of sintering temperature on dielectric, and impedance studies has been reported from a low (20 Hz) to a high frequency region (20 MHz) $SrMnO_3$ ceramic samples. The dielectric response revealed various electroactive regions in accordance with the Maxwell-Wagner model while the impedance analysis showed the dominant behaviour of microstructural grain boundaries. A possible combination of equivalent circuit was also proposed in order to determine the deviation from ideality. The circuits were also verified through frequency dependent conductivity response while the dependence of capacitance on temperature provided information on the possible ferroelectric behaviour.

1. INTRODUCTION

ABO_3-type complex perovskite ceramics with A as a divalent ion (Ca, Sr, and Ba) and B as a transition metal ion, are a subject of extensive research because of some associated astonishing properties like thermochromism (Heiras 2002), magnetoresistance (Bannikov 2008), magnetostructural and magnetoelectrical effects (Zeng 1999). The importance of these materials has increased manifold after the discovery of ferroelectricity, for example in $BaTiO_3$ which makes them feasible to utilize in capacitors and transducers (Shukla 2009, Fiebig 2004). In addition, high dielectric constants of these perovskites have further enhanced potential applicability in modern day technologies, especially by reducing the dimensions of electronic devices (Cava 2001).

Favourable electrical characteristics and high dielectric constant of perovskites depend upon many factors such as preparation techniques, ingredient's stoichiometry, structural crystallography and temperature effects. In this regard, nano-crystalline

perovskite ceramics have emerged as a class of materials which contains highly conducting grains along with conveniently placed resistive grain boundaries and suitable surface effects; all contributing towards beneficial electrical properties (Ehi-Eromosele 2016). To study the individual contributions of these electro active regions and their consequent effects on overall electrical behaviour of the materials, complex impedance spectroscopy (CIS) is used in which real and imaginary parameters of impedance are measured as a function of frequency or temperature. Being a powerful technique, it has extensively been used to characterize electrically volatile microstructural regions of the material by analysing, which resistive element, such as grains or grain boundaries, possesses the dominant behaviour. A parallel combination of the equivalent circuit is drawn to calculate the values of resistive (R) and capacitive (C) components of the circuit. This *RC* circuit generates one or more semicircles and thus the electro active regions are identified depending on the frequency range at which they are formed (Verma 2011). The distinction between these regions is fairly easy, except for the ferroelectric materials, which can also be separated from non-ferroelectric materials by temperature dependent capacitance response (Irvine 1990). Furthermore, the temperature dependent studies can reveal the activation or deactivation of the conduction mechanism, finds the localized or delocalized nature of charge carriers and estimates the hopping mechanism (Li 2012, Li 2011).

Recently, manganese based perovskite ceramics have been synthesized to study the possible occurrence of the electric and magnetic properties simultaneously which gives a magnetic degree of freedom operated by electric field or vice versa (Fiebig 2005, Sakai 2011). In addition to these multiferroic characteristics, occurrence of good electrical properties can make these materials applicable in dynamic random access memory capacitors and voltage controlled oscillators (Verma 2009).

In this research, we report the synthesis of strontium based manganese type perovskite through sol-gel auto-ignition technique using metal nitrates as precursors to study its dielectric and impedance characteristics. $SrMnO_3$ have been previously synthesized to study the catalytic and magnetic properties (Doroftei 2014, Battle 1988), while the first principle studies reveal the occurrence of ferroelectricity in this material at room temperature (Lee 2010). Thus, the study of electrical properties of this material is important in a sense that it could be a strong candidate for ferroelectric materials as predicted by theoretical studies. Furthermore, an attempt to calculate the Curie temperature using electrical properties may help the researchers to perform the ferroelectric measurements.

2. EXPERIMENTAL

Sol-gel auto-combustion technique is very feasible in making required phases of perovskite based oxide ceramics. It favors the formation of nano-crystallite structures in short interval of time. In order to prepare the $SrMnO_3$ samples using this technique, stoichiometrically weighed suitable amount of analytical grade salts i.e., strontium nitrate [$Sr(NO_3)_2.6H_2O$, ≥99%] and manganese nitrate [$Mn(NO_3)_2.6H_2O$, ≥97%] were dissolved in distilled water. Citric acid was added as a fuel agent for ignition reaction in molar ratio of 1 : 2, for metal nitrates to citric acid. All these analytical grade reagents were purchased from Sigma Aldrich (USA). The mixed solution was dried at temperature of 95 °C and stirred constantly with magnetic stirrer which led to the

formation of xerogel. At the instant, the temperature was increased up to 300 °C. After a while, a self-ignited combustion took place and xerogel was converted into a fine powder. The as-prepared powder was then sintered at different temperatures ranging from 600 to 1200 °C to make four different samples named as a, b, c and d. The powder samples were compressed into pellets having 10 mm diameter and ~1.5 mm thickness, using an Apex hydraulic press. Bruker D/8 Advance X-ray diffractometer (XRD) was used to find the accurate sintering temperature for the pure perovskite phase. The Precision Wayne Kerr 6500B Impedance Analyzer was used for the dielectric and impedance analysis at different temperatures.

3. RESULTS AND DISCUSSION

Crystalline phases of all the sintered ceramic samples were determined using XRD, as shown in Fig. 1. Formation of single phase hexagonal perovskite structure in the series of samples was not observed until the sample, sintered at 1000 °C for 4 hrs (Fig. 1c). The patterns of the samples sintered at 600 and 800 °C contained many impurity phases which include tetragonal phase of Mn_2O_3 (●), hexagonal phase of Sr (◊), in addition to hexagonal perovskite phase of $SrMnO_3$ (♥), as shown in Fig. 1(a & b). Impurity free hexagonal perovskite phase was developed by sintering the sample at 1000 °C for 4 hrs (Fig. 1c). Well-defined and sharp peaks, shown in Fig. 1c, matched perfectly with JCPDS no. 00-024-1213, a characteristic reference pattern of $SrMnO_3$, exhibiting hexagonal perovskite structure. Indexing of the pattern was performed using the indexing method for hexagonal structure as given by Cullity (Iqbal 2013). Further heating the sample at 1200 °C for 4 hrs, cause small intensity peaks to distort which shows that the perovskite phase is stable up to 1000 °C. Pure phase pattern was further studied by employing Rietveld's refinement technique to determine the difference plot between the observed pattern and formally calculated pattern. Refined diffraction pattern along with indexed intensity peaks have been shown in Fig. 2(a),

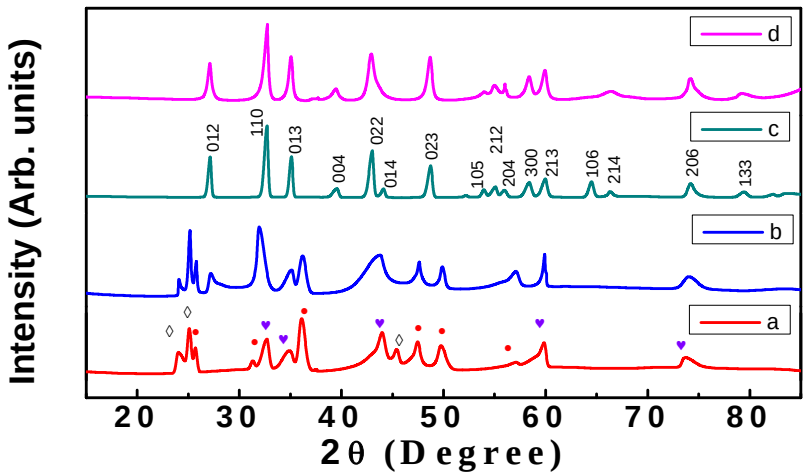

Fig. 1. XRD patterns of $SrMnO_3$ samples sintered at (a) 600 °C, (b) 800 °C, (c) 1000 °C, and (d) 1200 °C for 4 hrs each. Sample sintered at 600 °C and 800 °C contains Mn_2O_3 tetragonal phase (●), Sr hexagonal phase (◊) and $SrMnO_3$ hexagonal perovskite phase (♥)

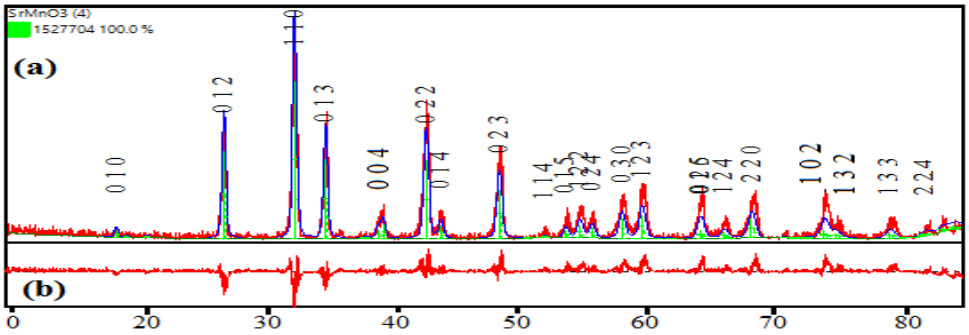

Fig. 2. (a) Rietveld refined pattern of $SrMnO_3$ sintered at 1000 °C for 4 hrs, (b) difference plot

while Fig. 2(b) depicts the difference of plot. In Rietveld's refinement, a model structure which has an approximately ideal pattern is required. To improve the fitting, profile parameters which included scale and occupancy factors, peak asymmetric, lattice and isothermal parameters were refined. The refinement was done with the P63/mmc space group for the hexagonal perovskite structure using the pseudo-Voigt function. A fairly good agreement was obtained between the peak positions of the calculated and the observed pattern but the intensities were found relatively odd. Refined structural parameters along with the residual factors are given in Table 1.

Temperature dependent dielectric response and tangent loss for the $SrMnO_3$ sample sintered at 1000 °C for 4 hrs has been shown in Fig. 3(a) and 3(b), respectively, determined in the temperature range of 70-280 °C. The dielectric parameters were studied on a large frequency range from 20 Hz to 20 MHz. A large dispersion for the dielectric constant and tangent loss can be seen at low frequencies, which decreases as the frequency is increased. This behaviour is best explained by the Maxwell-Wagner theory for the heterogeneous systems (Iqbal 2013). These types of systems contain grains which are separated by grain boundaries. The grains act as the conducting medium while the grain boundaries act as the resistive component, as explained by Koop (Koop 1951). When an electric field is applied to such a system, surface charges start to pile up at the interfaces between the grains and grain boundaries, resulting in interfacial polarization at the grain boundaries. When the frequency is low, these charges try to align themselves with the field but when the frequency becomes high,

Table 1 Refined structural parameters of $SrMnO_3$.

Structural Model	**Cell Parameters (Å)**		**Sites**	**Positional coordinates**			***R* factors**	
				x	*y*	*z*		
$P6_3/mmc$ (Hexagonal perovskite)	*a*	5.514	Sr1	0	0	0.12	R_{exp}	20.57
	b	5.514	Sr2	0.33	0.67	0.75	R_p	26.15
	c	9.15	Mn	0.33	0.67	0.113	R_{wp}	31.84
	V	241 $Å^3$	O1	0.5	0	0	χ^2	2.4
	D	147.3	O2	0.1821	0.364	0.25	R_b	16.7

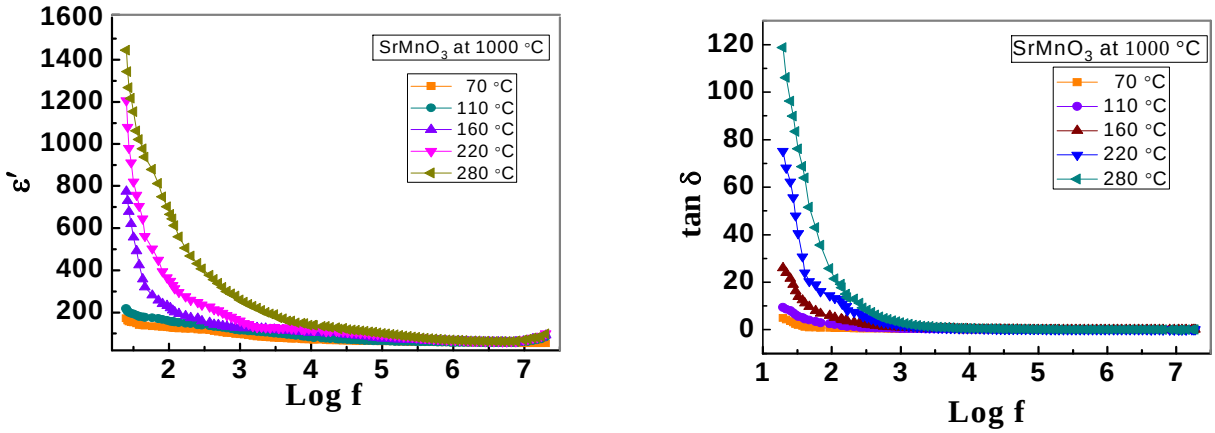

Fig. 3. Variation of dielectric constant (ε') and tangent loss (tanδ) with frequency at different temperatures for the $SrMnO_3$ sample sintered at 1000 °C for 4 hrs

these dipoles are not able to synchronize themselves with the changing field and thus low dielectric constant is obtained (Ali 2013). This means that grain boundaries have a dominant behaviour at low frequencies while the effect of grains persist at high frequencies. High resistance given by the grain boundaries at low frequency will require more energy for charge carriers to flow and thus the energy losses are also high in the low frequency region, as shown in the tangent loss plot in Fig. 3(b).

Fig. 4 demonstrates the variation of dielectric constant with temperature which reveals that dielectric constant strongly depends upon the temperature. The variation shows a gradual increase in the dielectric constant as the temperature is increased. This means that more charges accumulate at the interfaces, which cause an increase in the polarization value and thus permittivity increases. This increase in dielectric value leads us to a shift from the ferroelectric phase to a paraelectric phase as the temperature is increased (Sindhu 2012).

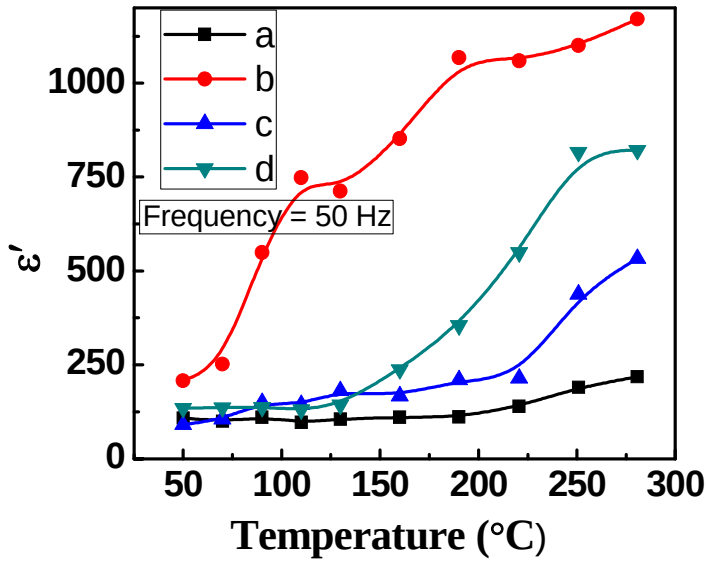

Fig. 4. Variation in dielectric constant (ε') with temperature at 50 Hz for all the samples

Fig. 5 shows a plot of *ac* conductivity as a response of frequency. The plot reveals a frequency independent *dc* component at low frequencies and a frequency dependent *ac* component at high frequencies. The independent region: where a straight line parallel to x-axis is achieved, simple *RC* elements are sufficient to demonstrate. For the frequency dependent region, an additional element is required to overcome the departures from the ideal Debye behaviour. For this purpose along with all the electrically active components, an additional constant phase element (CPE) is attached (Elliott 1977). The addition of CPE is not accidental, rather it describes the 'Jonsher power law' dependence of electrical components on frequency. The power law is given by:

$$\sigma_{ac} = A\omega^{s} \tag{1}$$

where ω is the frequency and A is a pre-exponential factor. The exponent s is the slope of the frequency dependent region in the *ac* conductivity plot (Fig. 5). Both A and s are temperature and material dependent while the values of s lie between 0 and 1. The exponent s demonstrates the interaction of mobile ions with lattice. When the value of s is zero, *ac* conductivity is independent of the frequency and no interaction between the ions and lattice takes place and thus the polaron hopping is zero which results in an ideal Debye behaviour. When the value of s increases, the conductivity becomes dependent on the frequency and polaron hopping is generated, resulting in non-Debye type behaviour. This process is best explained in terms of CBH (correlated barrier height) model in which conduction occurs due to hopping of polarons over a potential barrier which exists between the correlated sites. The energy required to cross

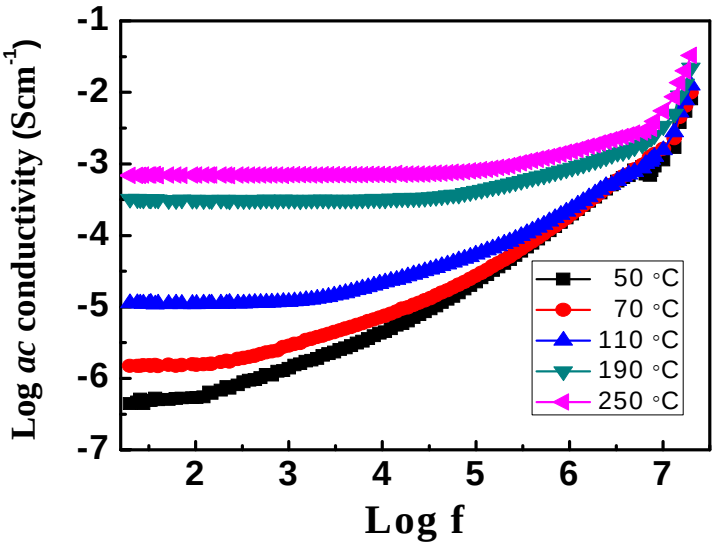

Fig. 5. Variation of *ac* conductivity with frequency (both in log scale) obtained at different temperatures for the sample sintered at 1000 ºC for 4 hrs

this barrier is called as binding energy. The equation relating the exponent and binding energy for this model is given as:

$$s = 1 - \frac{6kT}{[W + kT\ln(\omega\tau_0)]} \quad (2)$$

where *k* is Boltzmann constant, *T* is temperature and *W* is the binding energy. Fig. 6 shows the variation in the exponent *s* and binding energy *W* with temperature. It can be seen that as the temperature is increased, the value for *s* decreases, and large polaron hopping is produced for the conduction mechanism as the binding energy is also increasing (El-Sayed 2014, Bouzidia 2015).

Fig. 7 shows the increasing behaviour of the capacitance at 2 kHz frequency, as the temperature is increased, for the sample sintered at 1000 °C. This behaviour is in exact agreement with the variation of the dielectric constant whose behaviour is just the same (increasing with increasing temperature) as shown in Fig. 4. These plots are used in an attempt to clarify the ferroelectric Curie temperature of materials by obtaining a peak at T_c (Dhak 2008). It can be seen that the values of dielectric constant (Fig. 4) and capacitance (Fig. 7) are increasing and no characteristic peak is obtained at the given frequency range. This leads to estimate that the possible Curie temperature at around 325 °C. This is done by plotting the graph of inverse of capacitance with temperature (Fig. 8), thus approximating the ferroelectric to paraelectric phase transition temperature (West 1997).

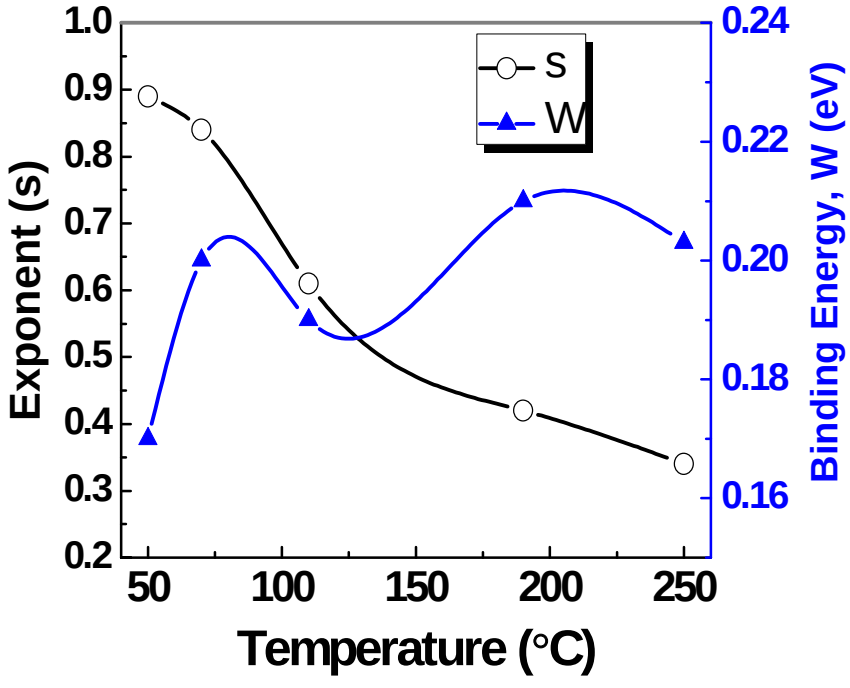

Fig. 6. Variation of exponent *s* and binding energy (W) with temperature for the sample sintered at 1000 ºC for 4 hrs

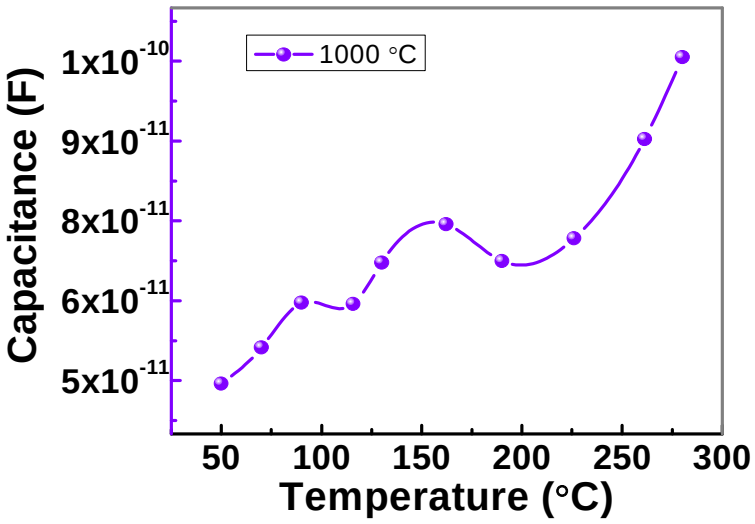

Fig. 7. Variation of capacitance with temperature for the sample sintered at 1000 °C for 4 hrs

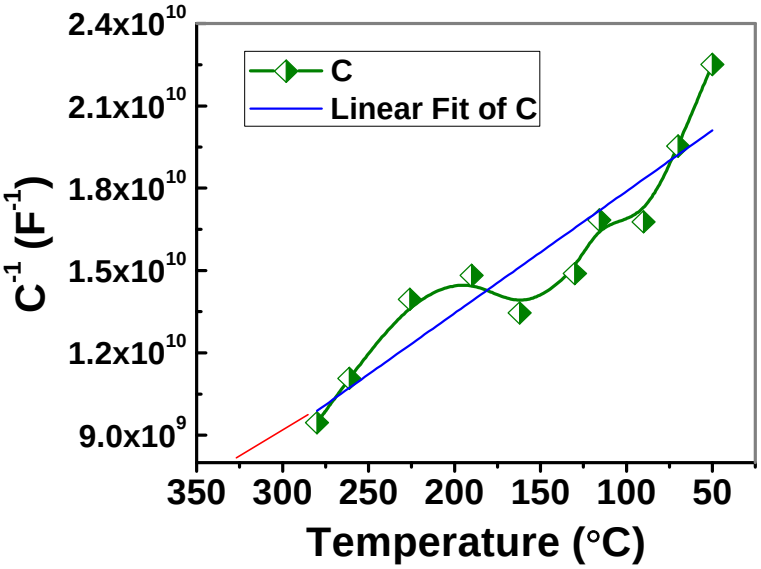

Fig. 8. Variation of inverse of capacitance with temperature for the sample sintered at 1000 ºC for 4 hrs. Linear fitting shows the intercept on temperature axis at around 325 °C

4. CONCLUSION

Phase pure synthesis of $SrMnO_3$ ceramic samples was optimized by varying the sintering temperature, in order to systematically investigate the structural, dielectric, conductive and resistive characteristics. XRD confirms the formation of hexagonal perovskite structure of the sample sintered at 1000 °C for 4 hrs. A gradual development of hexagonal perovskite structure has been observed with increasing sintering

temperature. Dielectric studies reveal a strong temperature dependent behavior. Complex impedance spectroscopy confirms the dominant electro-active regions based on the conduction variations within the grains and grain boundaries. The *ac* conductivity obeys Joshner's power law from which binding energy of the charge carries has been estimated in the range of 0.17 to 0.21 eV. These results suggest that conduction mechanism is $SrMnO_3$ can be explained by correlated barrier height (CBH) model. The electric Curie temperature of $SrMnO_3$ is determined as 325 °C using characteristic temperature dependent capacitance. Owing to interesting electrical properties, it is inferred that $SrMnO_3$ ceramics can be accounted for capacitors and non-volatile ferroelectric memory devices.

Acknowledgement: Authors are thankful to higher education commission of Pakistan (HEC) for financially supporting this work through research project number NRPU-2471.

REFERENCES

Ali, G., Siddiqi, S.A., Ramay, S.M., Atiq, S. and Saleem, M. (2013), "Effect of Co substitution on structural, electrical and magnetic properties of $Bi_{0.9}La_{0.1}FeO_3$ by sol-gel synthesis," *Int. J. Miner. Metall. Mater.*, **20** 166-170.

Bannikov, V.V., Shein, I.R., Kozhevnikov, V.L. and Ivanovskii, A.L. (2008), "Magnetism without magnetic ions in non-magnetic perovskites $SrTiO_3$, $SrZrO_3$ and $SrSnO_3$," *J. Magn. Magn. Mater.,* **320**, 936-942.

Battle, P.D., Gibb, T.C. and Jonnes, C.W. (1988), "The structural and magnetic properties of $SrMnO_3$: A reinvestigation," *J. Solid State Chem.*, **74** 60-66.

Bouzidia, C., Sdirib, N., Boukhachem, A., Elhouicheta, H. and Ferid, M. (2015), "Impedance analysis of $BaMo_{1-x}W_xO_4$ ceramics," *Superlattice. Microst.*, **82** 559-573.

Cava, R. (2001), "Dielectric materials for applications in microwave communications," *J. Mater. Chem.,* **11** 54–62.

Dhak, D., Dhak, P. and Pramanik, P. (2008), "Influence of substitution on dielectric and impedance spectroscopy of $Sr_{1-x}Bi_{2+y}Nb_2O_9$ ferroelectric ceramics synthesized by chemical route," *Appl. Surf. Sci.*, **254** 3078-3092.

Doroftei, C., Popa, P.D. and Rezlescu, E.N. (2014), "Nanocrystalline $SrMnO_3$ powder as catalyst for hydrocarbon combustion," *J. Alloy. Compd.*, **584** 195–198.

Ehi-Eromosele, C.O., Ita, B.I., Iweala, E.E.J., Ogunniran, K.O., Adekoya, J.A. and Ehi-Eromosele, F.E. (2016), "Structural and magnetic characterization of $La_{0.7}Sr_{0.3}MnO_3$ nanoparticles obtained by the citrate-gel combustion method: Effect of fuel to oxidizer ratio," *Ceram. Int.*, **42,** 636 – 642.

Elliott, S.R. (1977), "Theory of AC conduction in chalcogenide glasses," *Philos. Mag.*, **36** 1291-1304.

El-Sayed, K., Mohamed, M.B., Heiba, Z.K. and Al-Nabriss, A.R. (2014), "Structure, magnetic and dielectric properties of Se-xFe," *Superlattice. Microst.*, **75**, 311-323.

Fiebig, M., (2005), "Revival of the magnetoelectric effect," *J. Phys. D: Appl. Phys.*, **38** R123– R152.

Fiebig, M., Eremenko, V.V. and Chupis, I.E. *Magnetoelectric Interaction Phenomena in Crystals,* Kluwer Academic Publishers, The Netherlands, 2004, 334.

Heiras, J., Pichardo, E., Mehmood, A., Lopez, T. and Blanco, O. (2002), "Thermochromism in (Ba,Sr)-Mn oxides," *J. Phys. Chem. Solids,* **63**, 591-595.

Iqbal, M.A., Islam, M.U., Ali, I. and Khan, M.A. (2013), "High frequency dielectric properties of Eu^{+3}-substituted Li-Mg ferrites synthesized by sol-gel auto-combustion method," *J. Alloy. Compd.*, **586** 404-410.

Irvine, J.T.S., Sinclair, D.C. and West, A.R., (1990), "Electroceramics: characterization by impedance spectroscopy," *Adv. Mater.*, **2** 132-138.

Koop, C.G. (1951), "On the dispersion of resistivity and dielectric constant of some semiconductors at audio frequencies," *Phys. Rev.*, **83** 121.

Lee, J.H. and Rabe, K.M. (2010), "Epitaxial-strained-induced multiferroicity in $SrMnO_3$ from first principles," *Phys. Rev. Lett.*, **104** 207204.

Li, M. and Sinclair, D.C. (2012), "The extrinsic origin of high permittivity and its temperature and frequency dependence in $Y_{0.5}Ca_{0.5}MnO_3$ and $La_{1.5}Sr_{0.5}NiO_4$ ceramics," *J. Appl. Phys.*, **111** 054106.

Li, M., Sinclair, D.C. and West, A.R. (2011), "Extrinsic origin of the relaxorlike behavior in $CaCu_3Ti_4O_{12}$ ceramics at high temperatures: a cautionary tale," *J. Appl. Phys.*, **109** 084106.

Pawar, R.P. and Puri, V. (2014), "Structural, electrical and dielectric properties of $(Sr_{1-x}Ca_x)MnO_3$ $(0 \leq x \leq 1.0)$ ceramics," *Ceram. Int.*, **40**, 10424-10430.

Rout, S.K., Hussain, A., Lee, J.S., Kim, I.W. and Woo, S.I., (2009), "Impedance spectroscopy and morphology of $SrBi_4Ti_4O_{15}$ ceramics prepared by soft chemical method," *J. Alloy. Compd.*, **477** 706–711.

Sakai, H., Fujioka, J., Fukuda, T., Okuyama, D., Hashizume, D., Kagawa, F., Nakao, H., Murakami, Y., Arim, T., Baron, A.Q.R., Taguchi, Y. and Tokura, Y. (2011), "Displacement-Type Ferroelectricity with Off-Center Magnetic Ions in Perovskite $Sr_{1-x}Ba_xMnO_3$," *Phys. Rev. Lett.*, **107** 137601-5.

Shukla, A., Choudhary, R.N.P. and Thakur, A.K. (2009), "Thermal, structural and complex impedance analysis of Mn^{4+} modified $BaTiO_3$ electroceramic," *J. Phys. Chem. Solids*, **70** 1401–1407.

Sindhu, M., Ahlwat, N., Sanghi, S., Agarwal, A. and Ahlawat, N. (2012), "Reitveld refinement and impedance spectroscopy of calcium titanate," *Current Appl. Phys.*, **12** 1429-1435.

Verma, K.C., Kotnala, R.K., Mathpal, M.C., Thakur, N., Gautam, P. and Negi, N.S. (2009), "Dielectric properties of nanocrystalline $Pb_{0.8}Sr_{0.2}TiO_3$ thin films at different annealing temperatures," *Mater. Chem. Phys.*, **114** 576–579.

Verma, K.C., Ram, M., Singh, J. and Kotnala, R.K., (2011), "Impedance spectroscopy and dielectric properties of Ce and La substituted $Pb_{0.7}Sr_{0.3}(Fe_{0.012}Ti_{0.988})O_3$ nanoparticles," *J. Alloy. Compd.*, **509** 4967–4971.

West, A.R., Sinclair, D.C. and Hirose, N. (1997), "Characterization of electrical materials, especially ferroelectrics, by impedance spectroscopy," *J. Electroceram.*, **1** 65-71.

Zeng, Z. and Greenblatt, M.C. (1999), "Large magnetoresistance in antiferromagnetic $CaMnO_{3-\delta}$," *Phys. Rev. B,* **59** 8784-8788.